A Ca(v)3.2/syntaxin-1A signaling complex controls T-type channel activity and low-threshold exocytosis.

Norbert Weiss, Shahid Hameed, José Fernández-Fernández, Katell Fablet, Maria Karmazinova, Cathy Poillot, Juliane Proft, Lina Chen, Isabelle Bidaud, Arnaud Monteil, et al.

A $Ca_v3.2$/syntaxin-1A signaling complex controls T-type channel activity and low-threshold exocytosis

Norbert Weiss[1,2,3], Shahid Hameed[1], José M. Fernández-Fernández[4], Katell Fablet[2,3], Maria Karmazinova[5], Cathy Poillot[2,3], Juliane Proft[6], Lina Chen[1], Isabelle Bidaud[7,8,9,10], Arnaud Monteil[7,8,9,10], Sylvaine Huc-Brandt[7,8,9,10], Lubica Lacinova[5], Philippe Lory[7,8,9,10], Gerald W. Zamponi[1,§] and Michel De Waard[2,3,§]

From [1]Hotchkiss Brain Institute, Department of Physiology and Pharmacology, University of Calgary, T2N4N1 Calgary, Canada; [2]Grenoble Institute of Neuroscience, INSERM U836, 38706 La Tronche, France; [3]University Joseph Fourier, 38000 Grenoble, France; [4]Laboratory of Molecular Physiology and Channelopathies, Department of Experimental and Health Science, Universitat Pompeu Fabra, 08003 Barcelona, Spain; [5]Laboratory of Biophysics, Institute of Molecular Physiology and Genetics, Slovak Academy of Sciences, 83334 Bratislava, Slovakia; [6]Hotchkiss Brain Institute, Department of Clinical Neurosciences, University of Calgary, T2N4N1 Calgary, Canada; [7]Département de Physiologie, Institut de Génomique Fonctionnelle, 34094 Montpellier, France; [8]Unité Mixte de Recherche 5203, Centre National de la Recherche Scientifique, 34396 Montpellier, France; [9]Institut National de la Santé et de la Recherche Médicale U661, 34094 Montpellier, France; [10]Institut Fédératif de Recherche No. 3, Universités Montpellier I and II, 34090 Montpellier, France.

Running title: *Regulation of T-type Ca^{2+} channels by SNARE proteins*

[§]To whom correspondence should be addressed:
Dr. Gerald W. Zamponi: Hotchkiss Brain Institute, Department of Physiology and Pharmacology, University of Calgary, 1A25A Health Research & Innovation Center, 3330 Hospital Drive N.W, T2N 4N1 Calgary, Canada; Tel: 403-220-8687; Fax: 403-210-8106; Email: zamponi@ucalgary.ca
Dr. Michel De Waard, Grenoble Institute of Neurosciences, INSERM U836, Laboratory of Ion Channels, Functions and Pathologies, Bâtiment Edmond J. Safra, Chemin Fortuné Ferrini, 38706 La Tronche, France; Tel: +33 (0)4 56 52 05 63; Fax: +33 (0)4 56 52 06 37; Email: dewaardm@ujf-grenoble.fr

Keywords: calcium channel; T-type; $Ca_v3.2$ channel; SNARE; syntaxin-1A; SNAP-25; exocytosis; neuron; MPC cell

---

Background: T-type calcium channels play a unique role in low-threshold exocytosis.
Results: Syntaxin-1A interacts with the carboxy-terminus domain of $Ca_v3.2$ channels and modulates channel activity and low-threshold exocytosis.
Conclusion: Low-threshold exocytosis relies to a syntaxin-1A/T-type calcium channel signaling complex.
Significance: Elucidating the molecular mechanisms by which T-type channels control low-threshold exocytosis is crucial for understanding their implication in synaptic transmission.

ABSTRACT

T-type calcium channels represent a key pathway for Ca^{2+} entry near the resting membrane potential. Increasing evidence supports a unique role of these channels in fast and low-threshold exocytosis in an action potential-independent manner, but the underlying molecular mechanisms have remained unknown. Here, we report the existence of a syntaxin-1A/$Ca_v3.2$ T-type calcium channel signaling complex that relies on molecular determinants that are distinct from the synaptic protein interaction site (*synprint*) found in synaptic high-voltage-activated calcium channels. This interaction potently modulated $Ca_v3.2$ channel activity, by reducing channel availability. Other members of the T-type calcium channel family were also regulated by syntaxin-1A, but to a smaller extent. Overexpression of $Ca_v3.2$ channels in

MPC 9/3L-AH chromaffin cells induced low-threshold secretion that could be prevented by uncoupling the channels from syntaxin-1A. Altogether, our findings provide compelling evidence for the existence of a syntaxin-1A/T-type Ca^{2+} channel signaling complex and provide new insights into the molecular mechanism by which these channels control low-threshold exocytosis.

INTRODUCTION

Ca^{2+} entry through the high-voltage-activated (HVA) $Ca_v2.2$ (N-type) and $Ca_v2.1$ (P/Q-type) Ca^{2+} channels into presynaptic nerve terminals supports a transient Ca^{2+} microdomain that is essential for synaptic exocytosis (1-3). To ensure fast and efficient neurotransmitter release, the vesicle-docking / release machinery must be located near the source of Ca^{2+} entry. In many cases, this close localization is achieved by direct interaction of SNARE proteins with the Ca^{2+} channels (4-6). Indeed, syntaxin-1A/1B, SNAP-25 and synaptotagmin-1 specifically interact with $Ca_v2.1$ and $Ca_v2.2$ channels by binding to a synaptic protein interaction site (*synprint*) located within the intracellular II-III linker region of the channels (7-11), and disruption of Ca^{2+} channel-SNARE coupling alters neurotransmitter release (6,12,13). A perhaps equally important consequence of SNARE protein-Ca^{2+} channel interactions is the ability of SNARE proteins to modulate presynaptic Ca^{2+} channel activity, thus fine tuning the amount of Ca^{2+} that enters the synaptic terminal. Specifically, the binding of syntaxin-1A and SNAP-25 to $Ca_v2.1$ and $Ca_v2.2$ subunits shifts the voltage-dependence of inactivation toward more hyperpolarized membrane potentials to reduce channel availability (11,14-18), and this effect is modulated by other members of the vesicle release complex (15,16,19,20).

In contrast with HVA channels, low-voltage-activated (LVA) T-type Ca^{2+} channels represent an important source of Ca^{2+} entry near the resting membrane potential. It is established that T-type Ca^{2+} currents mediate low-threshold burst discharges that occur during physiological neuronal rhythmogenesis as well as during pathological states such as epilepsy (21), and that they regulate various cellular functions such as neuronal development, dendritic integration, sensory transmission or pain signaling (for review see (22)). Furthermore, there is an increasing body of evidence that T-type channels can trigger fast and low-threshold exocytosis (23-27). In contrast with HVA Ca^{2+} channels, all members of the T-type channel family (i.e., $Ca_v3.1$, $Ca_v3.2$ and $Ca_v3.3$) lack the *synprint* site, and it is unclear as to how T-type channels are coupled to the exocytosis process at the molecular level.

Here, we reveal the existence of a syntaxin-1A/$Ca_v3.2$ T-type Ca^{2+} channel complex in central neurons and show that this interaction involves different molecular determinants from those found in HVA channels. This interaction of syntaxin-1A with the $Ca_v3.2$ subunit potently modulates channel gating properties and appears essential for T-type channel-triggered low-threshold exocytosis.

EXPERIMENTAL PROCEDURES

Plasmid cDNA constructs-The cDNAs constructs used in this study were human $Ca_v3.1$, $Ca_v3.2$ and $Ca_v3.3$ (28,29), mouse syntaxin-1A (Stx-1A) and SNAP-25 subcloned in pcDNA3 vector. The pcDNA3 construct encoding for the botulinium neurotoxin C1 (BoNT/C1) was generously provided by Dr. Robert G. Tsushima and Dr. Herbert Gaisano. The Stx-1A construct lacking the transmembrane domain ($Stx1A^{\Delta TM}$, amino acids 1 to 265) in pCMV5 was kindly provided by Dr. Randy D. Blakely. The Stx1A"Open" in pMT2 was generated by mutating Leu^{165} and Glu^{166} to Ala as previously described (11).

Heterologous Expression and Electrophysiology-Human embryonic kidney tsA-201 cells were grown in a Dulbecco's modified Eagle's culture medium containing 10% fetal bovine serum and 1% penicillin/streptomycin (all products were purchased from Invitrogen) and maintained under standard conditions at 37°C in a humidified atmosphere containing 5% CO_2. Cells were transfected using the jetPEI™ transfection regent (Qbiogen, OH, USA) with either the $Ca_v3.1$, $Ca_v3.2$ or $Ca_v3.3$ channel, along with a green fluorescent protein (pEGFP, Clontech, CA, USA). Patch-clamp recordings were performed 48-72 hrs after transfection as previously described (30) in

the whole-cell configuration of the patch-clamp technique at room temperature (22-24°C) in a bathing medium containing (in millimolar): 5 $BaCl_2$, 5 KCl, 1 $MgCl_2$, 128 NaCl, 10 TEA-Cl, 10 D-glucose, 10 HEPES (pH 7.2 with NaOH). Patch pipettes were filled with a solution containing (in millimolar): 110 CsCl, 3 Mg-ATP, 0.5 Na-GTP, 2.5 $MgCl_2$, 5 D-glucose, 10 EGTA, 10 HEPES (pH 7.4 with CsOH), and had a resistance of 2-4 MΩ. Whole-cell patch-clamp recording were performed using an Axopatch 200B amplifier (Axon Instruments, Union City, CA). All traces were corrected on-line for leak currents, digitized at 10 KHz and filtered at 2 KHz. Intramembrane charge movement measurements were recorded using an HEKA-10 patch clamp amplifier (HEKA Electronic, Lambrecht, Germany). The extracellular solution contained (in millimolar): 105 CsCl, 10 HEPES, 10 D-glucose, 10 TEA-Cl, 2 $CaCl_2$, 1 $MgCl_2$ (pH 7.4 with CsOH). The intracellular solution contained (in millimolar): 130 CH_3SO_3Cs, 10 EGTA, 5 $MgCl_2$, 10 TEA-Cl, 5 Na-ATP, 10 HEPES (pH 7.4 with CsOH). 10 mM stock solution $ErCl_3$ (Sigma-Aldrich, St. Louis, MO, USA) was prepared daily in deionized water and diluted in the bath solution at a concentration of 30 μM prior to the experiment. Only the cells in which series resistance was below 5 MΩ were used for measurement of gating currents. Series resistance and capacitive transients were partly compensated by built-in circuits of the EPC 10 amplifier. Data were sampled at 10 kHz and filtered at 3 kHz. The linear component of the leak current and non-compensated capacitive transient was subtracted using the P/8 procedure. Total charge transferred during each pulse was evaluated by integrating the area below gating current trace at the beginning (Q_{on}) and after the end of each depolarizing pulse (Q_{off}). For capacitance measurements, MPC 9/3L-AH cells were transfected using Lipofectamine Plus (Invitrogen), as previously reported (6,31). The $Ca_v3.2$ channel was co-expressed with rat β_{2a} and rabbit $\alpha_2\delta$ subunits along with either the pEGFP, CD4-EGFP-$Ca_v3.2^{II\text{-}III}$ or CD4-EGFP-$Ca_v3.2^{Cter}$ construct, using a ratio of 1:1:1:0.6 respectively. Recordings were performed 48-72 hrs after transfection. The external solution contained (in millimolar): TEA-Cl 140, $CaCl_2$ 5, HEPES 10, D-glucose 10 (pH 7.3; 300 mosmoles/l) ($CaCl_2$ was omitted and 1mM EGTA was added for studies in 0 Ca^{2+}). Patch pipettes were filled with a solution containing (in millimolar): 13 CsCl, 120 CH_3CO_2Cs, 2.5 $MgCl_2$, 10 HEPES, 1 EGTA, 4 Na_2ATP, 0.1 Na_3GTP (pH 7.2; 295-300 mosmoles/l) and had a resistance of 2-4 MΩ. Capacitance measurements were performed using an EPC-10 patch-clamp amplifier using the "sine + dc" software lock-in amplifier method implemented in PatchMaster software. MPC 9/3L-AH cells were held at -90 mV except during membrane depolarization. The sinusoid had amplitude of 25 mV and a frequency of 1 kHz. The stimulation protocol consisted in a single depolarization to -20 mV for 80 ms. Single-pulse current data were leak-subtracted by hyperpolarizing sweeps. Capacitance changes in response to ionomycin were recorded from MPC 9/3L-AH cells transfected with either pEGFP or CD4-EGFP-$Ca_v3.2^{Cter}$ construct only. Ionomycin (1μM) was dissolved in the external solution indicated above and applied using a fast perfusion system (ALA VC^3-8SP; ALA Scientific Instruments, Inc., NY). Analysis was performed using Igor Pro software version 6.0 (Wavemetrics).

Co-immunoprecipitation experiments- Frozen rat brain tissue was homogenized in (10% w/v) of lysis buffer (in millimolar: 150 NaCl, 50 Tris, pH 7.5 and 1% NP-40 including a protease inhibitor cocktail (Roche)). The homogenate was centrifuged at ~16 000 *g* for 10 min at 4°C in a micro centrifuge and supernatant collected. For immunoprecepitation, 200 μL of aliquots of supernatant pre-cleared by addition of 40 μL of a 50% slurry (v/v) of rehydrated protein A-Sepharose beads (Amersham Pharmacia), followed by rotation at 4°C for 1 hr. Pre-cleared supernatants were then separately incubated with 5 μg of either anti-$Ca_v3.1$, anti-$Ca_v3.2$ or anti-$Ca_v3.3$ antibodies for 16 hrs at 4°C. To collect immuneprecipitated complex, the samples were further incubated for 2 hrs with 40 μL protein A-Sepharose beads (50% slurry). The beads with immunoprecipitated complex were washed four times with ice cold lysis buffer and resuspended in 40 μL of 2X SDS PAGE sample buffer. Heated at 70°C for 15 min and the soluble proteins were then resolved by SDS-PAGE and analyzed by Western blotting. Affinity-purified, rabbit polyclonal antibodies recognizing $Ca_v3.1$, $Ca_v3.2$ and $Ca_v3.3$

were purchased from Alomone Lab and mouse monoclonal syntaxin 1A antibody was from Chemicon International (Temecula, CA, USA). Co-immunoprecipitation experiments from tsA-201 cells were performed from cells expressing Stx1A-myc or SNAP-25 along with the CD4-EGFP-$Ca_v3.2^{Cter}$ fusion protein were solubilized with 400 µL of 50mM Tris/HCl pH 7.5, 0.05 mM EDTA and 10 mM Chaps Buffer supplemented with proteases inhibitor (1X, Roche) and lysed by sonication. Lysates were cleared by centrifugation at ~8000 *g* for 10 min. All steps were carried out on ice or at 4°C. Lysates were incubated for 3 hrs with 15 µL biotinylated anti-Myc antibody (Santa Cruz) or for 16 hrs with anti-GFP antibody (1/1000, Abcam) and then for 45 min with streptavidine beads or protein G beads (Invitrogen) at 4°C and were washed twice with PBS (1X) Tween 0.1% and twice with PBS (1X). The beads were finally resuspended in PBS (1X). Samples were resolved on Tris-glycine SDS-polyacrylamide gels and transferred to nitrocellulose membranes using standard methods. Membranes were blocked in 10% (w/v) milk in PBS (0.1% (v/v) Tween-20) and then incubated with either anti-GFP or anti-SNAP-25 primary antibodies for 2 hrs at room temperature. After being washing once for 5 min, membranes were incubated with horseradish peroxidase conjugated protein A (Abcam). The washed membranes were developed using enhanced chemiluminescence.

nRT culture, immunostaining and confocal imaging-The Nucleus reticularis area was isolated from lateral thalamus of P0-P1 rat pups, cut into small pieces and then digested in containing papain (Worthington, LS003126) culture media. After digestion, the tissue was washed and triturated for neuron dissociation. nRT neurons were seeded at low density onto coverslips pretreated with poly-D-lysine (Sigma, P7280) followed by Laminin (Sigma, L2020) in 24-well plate. Culture medium consisted of BME (Invitrogen, 21010) supplemented with 1% B-27 supplement (Invitrogen, 17504-044), 2mM L-glutamine (Invitrogen, 25030-049), 1mM sodium pyruvate (Invitrogen, 11360-070), 10 mM HEPES(Sigma, H7523), 0.6% D-glucose (Sigma, G7528), 1% pen strep (Invitrogen, 15140), and 5% fetal bovine serum (Invitrogen, 26140). The next day after plating, the existing media was replaced by fresh culture media, after that every 4-5 days half of the media was removed and replaced by fresh culture media. For immunostaining, cells were fixed with 4% paraformaldehyde in PBS for 20 min at room temperature, washed and permeabilized in PBST (PBS containing 0.02% Triton X-100) for 3 min, and blocked with blocking buffer (3% BSA in PBS) for 30 min. Cells were then incubated overnight at 4°C with primary polyclonal rabbit anti-$Ca_v3.2$ (Alomone) and mouse monoclonal anti-syntaxin-1A (Sigma) antibodies diluted at 1:400 and 1:500, respectively, in blocking buffer. Cells were then washed, incubated 1h at room temperature with anti-rabbit Alexa488-conjugated and anti-mouse Alexa555-conjugated secondary antibodies, washed and mounted on glass slide. Confocal images were acquired with a Zeiss LSM510 Meta microscope and analysed using ImageJ software. The intensity correlation analysis was performed using the ImageJ plugin previously described (32).

Statistics-Data values are presented as mean ± S.E.M. for *n* recorded cells. Statistical significance was determined using Student's *t* test: $^{*}p < 0.05$; $^{**}p < 0.01$; $^{***}p < 0.001$; NS, statistically not different.

RESULTS

Syntaxin-1A associates with $Ca_v3.2$ channels in central neurons - The existence of a relationship between T-type Ca^{2+} channels and neurotransmitter release (23-26) prompted us to examine the possible colocalization of these channels with SNARE proteins in central neurons. Isolated rat reticular thalamic neurons (nRT) that are known to express predominantly the $Ca_v3.2$ isoform of T-type channels (33) were immunolabeled, and T-type channel and syntaxin-1A distribution analyzed by confocal microscopy. The anti-$Ca_v3.2$ antibody labeling (green) revealed a somatodendritic pattern consistent with previous electrophysiological studies (34-36). Interestingly, intense syntaxin-1A labeling was also similarly observed along the somatodendritic axis (red) and visual inspection of the overlaid images and co-localized pixels suggests colocalization of the proteins (Fig. 1A). We used the intensity correlation analysis (ICA) method to test for a

staining relation between $Ca_v3.2$ channel and syntaxin-1A as previously described (32). The ICA plots of $Ca_v3.2$ and syntaxin-1A performed both on the soma and on dendrite regions were strongly skewed toward positive values (Fig. 1B), consistent with a highly dependent staining pattern. Furthermore, the calculated intensity correlation quotient values (ICQ) were positive and highly significant (+0.30 ± 0.01 and +0.31 ± 0.01 for the soma and dendrite respectively (n = 12; $p < 0.001$). These data thus strongly suggest that a pool of syntaxin-1A and $Ca_v3.2$ channels are present at the same subcellular level. We then investigated by co-immunoprecipitations whether T-type calcium channels and syntaxin-1A associate with each other at the protein level. As shown in Figure 1B, specific anti-$Ca_v3.1$, $Ca_v3.2$ and $Ca_v3.3$ antibodies precipitated syntaxin-1A from rat brain homogenate, thus suggesting the existence of T-type Ca^{2+} channel/syntaxin-1A complexes (Fig. 1C).

Syntaxin-1A modulates $Ca_v3.2$ channel activity - To investigate the impact of the $Ca_v3.2$/syntaxin-1A interaction on channel function, channel properties were analyzed in the absence and the presence of syntaxin 1A using whole-cell patch-clamp. The co-expression of syntaxin-1A with $Ca_v3.2$ channel in tsA-201 cells reveals a potent syntaxin-1A regulation of the voltage-dependence of T-type channel inactivation (Fig. 2A-C and Table S1). In syntaxin-1A expressing cells, the half-inactivation potential of $Ca_v3.2$ channels was shifted to more hyperpolarized potentials by -16.3 ± 1.2 mV ($p < 0.001$) (to -86.9 ± 1.2 mV, n = 28) compared to control cells (-70.6 ± 0.5 mV, n = 27). The syntaxin-1A-mediated modulation of $Ca_v3.2$ inactivation was abolished upon cleavage of syntaxin-1A by co-expression of the botulinium neurotoxin C1 (BoNT/C1) (Fig. 2C and Table S1), indicating that the membrane insertion domain of syntaxin-1A was necessary for the observed functional effects. Consistent with this observation, co-expression of a syntaxin-1A construct lacking the transmembrane domain was unable to modulate $Ca_v3.2$ channel inactivation (Fig. 2C and Table S1). Similar results were obtained with $Ca_v3.1$ and $Ca_v3.3$ channels, indicating that syntaxin-1A regulation is conserved across the entire T-type channel family (Fig. S1).

It is well established that syntaxin-1A exists in both "open" and "closed" conformations (37), and that syntaxin-1A state is an important determinant of N-type channel modulation (11). Similar to previous observations in N-type channels, co-expression of a mutant syntaxin-1A construct that is locked permanently in the "open" conformation failed to induce a hyperpolarizing shift of the steady-state in half-inactivation potential (Fig. 2C), indicating that syntaxin-1A mediated modulation of $Ca_v3.2$ channel is syntaxin state-dependent.

Besides regulating the voltage-dependence of $Ca_v3.2$ channel inactivation, syntaxin-1A also produced moderate effects on other gating properties of the channel, including a -5.7 mV hyperpolarizing shift of the activation curve (from -38.6 ± 0.6 mV (n = 31) to -44.2 ± 0.8 mV (n = 18), $p < 0.001$) (Fig. 2D and Table S1), a 1.6-fold slowing of the time constant of inactivation kinetics (from 13.1 ± 0.7 ms (n = 31) to 21.0 ± 1.3 ms (n = 18) at -20 mV, $p < 0.001$) (Table S1), and a 1.8-fold slowing of the time constant for recovery from fast inactivation (from 489.4 ± 25.9 ms (n = 25) to 876.3 ± 60.7 ms (n = 14), $p < 0.001$) (Table S1). In contrast, the voltage-dependence and kinetics of intramembrane charge movements of $Ca_v3.2$ channel were found unaffected upon co-expression of syntaxin-1A (Fig. S2). Unlike syntaxin-1A, co-expression of other synaptic proteins such as SNAP-25, synaptobrevin-1 and 2, CSP and Rim-1 produced only minor effects on $Ca_v3.2$ channel activity (Table S1). Altogether, our data indicate that syntaxin-1A is a robust and selective modulator of T-type Ca^{2+} channel inactivation.

Syntaxin-1A interacts within the carboxy-terminal domain of the $Ca_v3.2$ subunit - Previous studies have shown that functional interaction of N- and P/Q-type Ca^{2+} channels can be disrupted by a peptide containing the *synprint* site (12,13). In order to investigate the $Ca_v3.2$ molecular determinants of syntaxin-1A regulation, we examined the capability of the different intracellular regions of the $Ca_v3.2$ subunit to prevent syntaxin-1A regulation. T-type $Ca_v3.2$ channels were coexpressed in tsA-201 cells along

with syntaxin-1A +/- a construct in which the major intracellular regions of the channels were fused to a CD4 epitope as well as the green fluorescent protein (EGFP) (Fig. 3A). Barium currents were recorded at -20 mV from a holding potential of -85 mV (where 56% of the channels are tonically inactivated in the presence of syntaxin-1A *versus* 11% in the absence of syntaxin-1A) before and after a 5 sec hyperpolarizing prepulse to -130 mV. A 5 sec hyperpolarizing prepulse to -130 mV produced a 2.1-fold increase in current amplitude in cells expressing syntaxin-1A (*versus* 1.1-fold increase in the absence of syntaxin-1A) due to the recovery of channels from inactivation (Fig. 3B). This prepulse-induced current facilitation was found significantly decreased upon co-expression of the CD4-EGFP-$Ca_v3.2^{Cter}$ fusion protein (from 2.1 ± 0.2-fold (n = 20) to 1.4 ± 0.1 (n = 17), $p < 0.001$), whereas expression of the CD4-EGFP-$Ca_v3.2^{Cter}$ construct by itself did not affect Ba^{2+} currents in the absence of syntaxin-1A (indicating that the CD4-EGFP-$Ca_v3.2^{Cter}$ construct by itself does not alter the voltage-dependence of inactivation of $Ca_v3.2$ channels) (Fig. 3B). In contrast, expression of the other intracellular regions of the channel failed to prevent syntaxin-1A regulation (Fig. 3B), suggesting a potential interaction of syntaxin-1A within the carboxy-terminus of the channel. Consistent with a possible specific binding of syntaxin-1A within the C-terminal domain of $Ca_v3.2$, co-expression of syntaxin-1A in COS cells promoted translocation of a EGFP-$Ca_v3.2^{Cter}$ fusion protein to the plasma membrane whereas the EGFP-$Ca_v3.2^{II\text{-}III\ linker}$ fusion protein remained diffusely expressed inside the cell (Fig. 3C). The trafficking study was performed on COS cells because they present the advantage to have a smaller nucleus than tsA-201 cells and more diffuse cytoplasm, allowing a better analysis of protein trafficking and plasma membrane staining. Finally, co-immunoprecipitation experiments from tsA-201 cells using the CD4-EGFP-$Ca_v3.2^{Cter}$ fusion protein revealed that syntaxin-1A specifically interacts with the carboxy-terminus domain of the $Ca_v3.2$ subunit (Fig. 3D), which is in stark contrast with the reported syntaxin-1A interaction site on HVA channels (II-III loop). Altogether, these findings demonstrate that syntaxin-1A modulates $Ca_v3.2$ channel activity by interacting within the C-terminal domain of the channel and that co-expression of the putative interaction site of the channel competitively inhibits syntaxin-1A-induced channel modulation.

Like syntaxin-1A, SNAP-25 was also found to associate with the $Ca_v3.2$ C-terminus (Fig. S3). While SNAP-25 by itself produced only slight effects on T-type channel activity, its co-expression reversed the effects of syntaxin-1A on channel inactivation properties (Fig. S3 and Table S1), in analogy with previous observations with N-type channels (15,16).

$Ca_v3.2$-SNARE complexes contribute to low-threshold exocytosis - Besides conferring a regulation of channel availability, the interaction between syntaxin-1A and T-type channels may also serve as a means for optimizing the coupling between T-type channel-mediated Ca^{2+} entry and secretion. To test for this possibility, $Ca_v3.2$ channels were over-expressed in MPC 9/3L-AH cells, a chromaffin cell line already fully endowed with the vesicle release machinery, but devoid of voltage-gated Ca^{2+} channels (6). Voltage-dependent exocytosis was evaluated by monitoring membrane capacitance changes (indicative of vesicle fusion) in response to a 100 ms depolarizing step to -20 mV from a holding potential of -90 mV. Voltage-dependent activation of over-expressed $Ca_v3.2$ channels produced a robust increase in exocytosis (estimated by normalizing capacitance changes by Ca^{2+} charge density) which was reduced by 96% ($p < 0.001$) when SNARE proteins were uncoupled from the channel by co-expression of the CD4-EGFP-$Ca_v3.2^{Cter}$ fusion protein (Fig. 4C-D), even though Ca^{2+} entry *per se* was not affected (1.9 ± 0.7 pC/pF, (n = 10) *versus* 1.8 ± 0.4 pC/pF, (n = 15)) (Fig. 4A-B). In contrast, co-expression of the CD4-EGFP-$Ca_v3.2^{II\text{-}III\ linker}$ fusion protein, which does not interact with syntaxin-1A, had no effect on $Ca_v3.2$-induced voltage-dependent exocytosis. The observation that Ca^{2+} entry was not affected upon co-expression of the CD4-EGFP-$Ca_v3.2^{Cter}$ fusion protein is consistent with the notion that syntaxin-1A modulation is abolished when $Ca_v3.2$ channels are functionally coupled to a full SNARE complex.

To confirm that the decrease in exocytosis observed upon expression of the CD4-EGFP-$Ca_v3.2^{Cter}$ fusion protein is due to the uncoupling of

$Ca_v3.2$ channels from endogenous SNARE proteins and not to a direct distortion of the vesicle release machinery, exocytosis was evaluated in EGFP- and CD4-EGFP-$Ca_v3.2^{Cter}$-expressing MPC 9/3L-AH cells (in the absence of $Ca_v3.2$ channel) in response to a Ca^{2+} ionophore. Exposition of EGFP-expressing cells to ionomycin (1 µM) elicited an increase in membrane capacitance that was significantly reduced by 94% ($p < 0.001$) after removal of extracellular Ca^{2+} (273 ± 95 fF, (n = 13) *versus* 17 ± 11 fF, (n = 9)) (Fig. 5A-B). However, neither the magnitude (273 ± 95 fF, (n = 13) *versus* 288 ± 81 fF, (n = 11), $p = 0.37$), nor the kinetic (tau) of the exocytosis response (9.0 ± 2.1 sec *versus* 8.9 ± 1.9 sec, $p = 0.98$) was affected by overexpression of the CD4-GFP-$Ca_v3.2^{Cter}$ construct (Fig. 5A-C). These results indicate that the negative impact of the CD4-EGFP-$Ca_v3.2^{Cter}$ fusion protein on the voltage-dependent exocytosis from MPC 9/3L-AH cells expressing $Ca_v3.2$ channels is not due to a direct distortion of the exocytotic machinery by the fusion protein but rather to the uncoupling of the channel from endogenous SNARE proteins.

Altogether, these findings indicate that $Ca_v3.2$ channels have the propensity to support low-threshold exocytosis, and that this process requires a close proximity between the vesicle release machinery and the channel.

DISCUSSION

In the present study, we provide compelling evidence for the existence of a syntaxin-1A/$Ca_v3.2$ T-type Ca^{2+} channel signaling complex. We demonstrate that this interaction not only potently modulates $Ca_v3.2$ channel gating but also regulates T-type channel mediated exocytosis.

It was previously shown that $Ca_v2.1$ and $Ca_v2.2$ Ca^{2+} channels colocalize with syntaxin-1A at presynaptic nerve terminals (38-40) and that these channels can be isolated as a complex with SNARE proteins (41-43). We show that similarly to $Ca_v2.1$ and $Ca_v2.2$ channels, $Ca_v3.2$ channels also colocalize with syntaxin-1A along the somatodendritic axis of nRT neurons, and that these two proteins can be co-immunoprecipitated, thus suggesting the existence of a native syntaxin-1A/$Ca_v3.2$ channel signaling complex. Moreover, *in vitro* binding experiments indicate that syntaxin-1A interacts within the carboxy-terminal domain of the $Ca_v3.2$ subunit, which indicates that T-type channels use different structural determinants compared with the *synprint* site utilized by members of the HVA channel family. At this point it is unclear whether distinct syntaxin-1A structural determinants are involved in the interactions with Ca_v3 and Ca_v2 channels.

Electrophysiological analyses of $Ca_v3.2$ channels in tsA-201 cells revealed that syntaxin-1A potently decreases channel availability by shifting the steady-state inactivation toward more hyperpolarized potentials. This is qualitatively similar to what has been reported for N- and P/Q-type Ca^{2+} channels. Our observation that co-expression of the carboxy-terminal region of the $Ca_v3.2$ subunit prevents syntaxin-1A-mediated modulation of $Ca_v3.2$ channel strongly suggest that syntaxin-1A modulates channel activity by virtue of its direct binding to the carboxy-terminal of the $Ca_v3.2$ subunit, rather than the mere presence of a syntaxin-1A molecule in the cell. The notion that syntaxin-1A-mediated modulation of $Ca_v3.2$ channel inactivation is abolished by botulinium neurotoxin C1 or upon deletion of the syntaxin-1A transmembrane domain indicates that membrane anchoring of syntaxin-1A is critical for channel modulation, and is analogous with previous observations on HVA channels (44). The inability of the "open" form of syntaxin-1A to alter T-type channel gating also parallels previous observations in $Ca_v2.2$ (11). Given that syntaxin-1A undergoes a conformational switch from a "closed" state to an "open" during the vesicle release cycle (37,45,46), this suggests the possibility that syntaxin-1A may be able to dynamically regulate $Ca_v3.2$ channel availability during various stages of exocytosis. The observation that SNAP-25 coexpression could reverse the syntaxin-1A mediated effect on channel gating is reminiscent of findings with $Ca_v2.2$ (but not $Ca_v2.1$) channels (14-16). At this point, we do not know whether this is due to a direct competition between SNAP-25 and syntaxin-1A for the same binding site within the C-terminus region of the channel, or whether both proteins can bind to the channel simultaneously. Irrespective of these structural information, the syntaxin-1A mediated alteration in the voltage-dependence of inactivation and the ability of SNAP-25 to regulate this process may represent an important regulatory pathway for T-type Ca^{2+} channels. This is further

underscored when considering that these channels are ~50% inactivated near neuronal resting membrane potentials such that even small changes in the voltage dependence of inactivation can bring about dramatic changes in Ca^{2+} entry (47).

Besides modulating T-type Ca^{2+} channel gating, the physical association between $Ca_v3.2$ channel and SNARE proteins may contribute significantly to optimize $Ca_v3.2$-mediated exocytosis. Consistent with previous studies showing that $Ca_v2.1$, $Ca_v2.2$ or $Ca_v3.1$ channels can trigger voltage-dependent exocytosis when heterologously expressed in MPC-9/3L cells (6,31,48), we show that expression of $Ca_v3.2$ channel in these cells induced robust voltage-dependent exocytosis that was drastically reduced when SNARE proteins were competitively uncoupled from the channel by co-expression of the carboxy-terminal domain of the $Ca_v3.2$ subunit. This result is consistent with previous studies showing that disruption of N- and P/Q-type Ca^{2+} channels-SNAREs interaction by a peptide containing the *synprint* site prevents neurotransmitter release (12,13). It was proposed that uncoupling of Ca^{2+} channels from SNARE proteins may not only lead to a spatial dissociation of vesicles and channels, but also to a loss of feedback regulation that collectively alter exocytosis efficiency (49,50). In this context, our data fit with the idea that T-type Ca^{2+} channels support low-threshold exocytosis by virtue of their close association with the SNARE protein machinery. Such tight coupling may be particularly important for T-type channels due to their small unitary conductance and low open probability.

In conclusion, although HVA and T-type channels utilize completely different channel structural determinants for their interactions with the SNARE machinery, they are functionally regulated by syntaxin-1A in a strikingly similar manner. This may perhaps underscore the fundamental evolutionary importance for providing tight control over (and localizing the exocytosis machinery close to the source of) Ca^{2+} entry. Overall, our findings reveal unrecognized new insights into the regulation of T-type Ca^{2+} channels by SNARE proteins and provide the first molecular mechanism by which these channels contribute to low-threshold exocytosis.

REFERENCES

1. Llinas, R., Sugimori, M., and Silver, R. B. (1992) *Science* **256**, 677-679
2. Neher, E., and Sakaba, T. (2008) *Neuron* **59**, 861-872
3. Weber, A. M., Wong, F. K., Tufford, A. R., Schlichter, L. C., Matveev, V., and Stanley, E. F. (2010) *Nat Neurosci* **13**, 1348-1350
4. Jarvis, S. E., and Zamponi, G. W. (2001) *Trends Pharmacol Sci* **22**, 519-525
5. Zamponi, G. W. (2003) *J Pharmacol Sci* **92**, 79-83
6. Harkins, A. B., Cahill, A. L., Powers, J. F., Tischler, A. S., and Fox, A. P. (2004) *Proc Natl Acad Sci U S A* **101**, 15219-15224
7. Sheng, Z. H., Rettig, J., Takahashi, M., and Catterall, W. A. (1994) *Neuron* **13**, 1303-1313
8. Rettig, J., Sheng, Z. H., Kim, D. K., Hodson, C. D., Snutch, T. P., and Catterall, W. A. (1996) *Proc Natl Acad Sci U S A* **93**, 7363-7368
9. Kim, D. K., and Catterall, W. A. (1997) *Proc Natl Acad Sci U S A* **94**, 14782-14786
10. Sheng, Z. H., Yokoyama, C. T., and Catterall, W. A. (1997) *Proc Natl Acad Sci U S A* **94**, 5405-5410
11. Jarvis, S. E., Barr, W., Feng, Z. P., Hamid, J., and Zamponi, G. W. (2002) *J Biol Chem* **277**, 44399-44407
12. Mochida, S., Sheng, Z. H., Baker, C., Kobayashi, H., and Catterall, W. A. (1996) *Neuron* **17**, 781-788
13. Rettig, J., Heinemann, C., Ashery, U., Sheng, Z. H., Yokoyama, C. T., Catterall, W. A., and Neher, E. (1997) *J Neurosci* **17**, 6647-6656
14. Bezprozvanny, I., Scheller, R. H., and Tsien, R. W. (1995) *Nature* **378**, 623-626
15. Wiser, O., Bennett, M. K., and Atlas, D. (1996) *Embo J* **15**, 4100-4110
16. Zhong, H., Yokoyama, C. T., Scheuer, T., and Catterall, W. A. (1999) *Nat Neurosci* **2**, 939-941
17. Jarvis, S. E., Magga, J. M., Beedle, A. M., Braun, J. E., and Zamponi, G. W. (2000) *J Biol Chem* **275**, 6388-6394
18. Sutton, K. G., McRory, J. E., Guthrie, H., Murphy, T. H., and Snutch, T. P. (1999) *Nature* **401**, 800-804
19. Jarvis, S. E., and Zamponi, G. W. (2001) *J Neurosci* **21**, 2939-2948
20. Wiser, O., Tobi, D., Trus, M., and Atlas, D. (1997) *FEBS Lett* **404**, 203-207
21. Khosravani, H., and Zamponi, G. W. (2006) *Physiol Rev* **86**, 941-966
22. Cueni, L., Canepari, M., Adelman, J. P., and Luthi, A. (2009) *Pflugers Arch* **457**, 1161-1172
23. Carabelli, V., Marcantoni, A., Comunanza, V., de Luca, A., Diaz, J., Borges, R., and Carbone, E. (2007) *J Physiol* **584**, 149-165
24. Ivanov, A. I., and Calabrese, R. L. (2000) *J Neurosci* **20**, 4930-4943
25. Pan, Z. H., Hu, H. J., Perring, P., and Andrade, R. (2001) *Neuron* **32**, 89-98
26. Egger, V., Svoboda, K., and Mainen, Z. F. (2003) *J Neurosci* **23**, 7551-7558
27. Tang, A. H., Karson, M. A., Nagode, D. A., McIntosh, J. M., Uebele, V. N., Renger, J. J., Klugmann, M., Milner, T. A., and Alger, B. E. (2011) *J Neurosci* **31**, 13546-13561
28. Vitko, I., Bidaud, I., Arias, J. M., Mezghrani, A., Lory, P., and Perez-Reyes, E. (2007) *J Neurosci* **27**, 322-330
29. Baumgart, J. P., Vitko, I., Bidaud, I., Kondratskyi, A., Lory, P., and Perez-Reyes, E. (2008) *PLoS One* **3**, e2976
30. Weiss, N., Sandoval, A., Felix, R., Van den Maagdenberg, A., and De Waard, M. (2008) *Pflugers Arch* **457**, 315-326
31. Serra, S. A., Cuenca-Leon, E., Llobet, A., Rubio-Moscardo, F., Plata, C., Carreno, O., Fernandez-Castillo, N., Corominas, R., Valverde, M. A., Macaya, A., Cormand, B., and Fernandez-Fernandez, J. M. (2010) *Proc Natl Acad Sci U S A* **107**, 1672-1677

32. Li, Q., Lau, A., Morris, T. J., Guo, L., Fordyce, C. B., and Stanley, E. F. (2004) *J Neurosci* **24**, 4070-4081
33. Huguenard, J. R., and Prince, D. A. (1992) *J Neurosci* **12**, 3804-3817
34. Cueni, L., Canepari, M., Lujan, R., Emmenegger, Y., Watanabe, M., Bond, C. T., Franken, P., Adelman, J. P., and Luthi, A. (2008) *Nat Neurosci* **11**, 683-692
35. Joksovic, P. M., Bayliss, D. A., and Todorovic, S. M. (2005) *J Physiol* **566**, 125-142
36. McKay, B. E., McRory, J. E., Molineux, M. L., Hamid, J., Snutch, T. P., Zamponi, G. W., and Turner, R. W. (2006) *Eur J Neurosci* **24**, 2581-2594
37. Dulubova, I., Sugita, S., Hill, S., Hosaka, M., Fernandez, I., Sudhof, T. C., and Rizo, J. (1999) *Embo J* **18**, 4372-4382
38. Cohen, M. W., Jones, O. T., and Angelides, K. J. (1991) *J Neurosci* **11**, 1032-1039
39. Westenbroek, R. E., Hell, J. W., Warner, C., Dubel, S. J., Snutch, T. P., and Catterall, W. A. (1992) *Neuron* **9**, 1099-1115
40. Westenbroek, R. E., Sakurai, T., Elliott, E. M., Hell, J. W., Starr, T. V., Snutch, T. P., and Catterall, W. A. (1995) *J Neurosci* **15**, 6403-6418
41. Bennett, M. K., Calakos, N., and Scheller, R. H. (1992) *Science* **257**, 255-259
42. Leveque, C., el Far, O., Martin-Moutot, N., Sato, K., Kato, R., Takahashi, M., and Seagar, M. J. (1994) *J Biol Chem* **269**, 6306-6312
43. Yoshida, A., Oho, C., Omori, A., Kuwahara, R., Ito, T., and Takahashi, M. (1992) *J Biol Chem* **267**, 24925-24928
44. Bezprozvanny, I., Zhong, P., Scheller, R. H., and Tsien, R. W. (2000) *Proc Natl Acad Sci U S A* **97**, 13943-13948
45. Fiebig, K. M., Rice, L. M., Pollock, E., and Brunger, A. T. (1999) *Nat Struct Biol* **6**, 117-123
46. Richmond, J. E., Weimer, R. M., and Jorgensen, E. M. (2001) *Nature* **412**, 338-341
47. Tscherter, A., David, F., Ivanova, T., Deleuze, C., Renger, J. J., Uebele, V. N., Shin, H. S., Bal, T., Leresche, N., and Lambert, R. C. (2011) *J Physiol* **589**, 1707-1724
48. Harkins, A. B., Cahill, A. L., Powers, J. F., Tischler, A. S., and Fox, A. P. (2003) *J Neurophysiol* **90**, 2325-2333
49. Mochida, S., Westenbroek, R. E., Yokoyama, C. T., Zhong, H., Myers, S. J., Scheuer, T., Itoh, K., and Catterall, W. A. (2003) *Proc Natl Acad Sci U S A* **100**, 2819-2824
50. Keith, R. K., Poage, R. E., Yokoyama, C. T., Catterall, W. A., and Meriney, S. D. (2007) *J Neurosci* **27**, 265-269

FOOTNOTES

Acknowledgments - We are grateful to Drs. Robert G. Tsushima (York University, Toronto, Canada) and Herbert Gaisano (University of Toronto, Toronto, Canada) for providing the BoNT/C1, and to Dr. Randy D. Blakeley (Vanderbilt University, Nashville, USA) for the Stx1A$^{\Delta TM}$ constructs. We thank Dr. Amy Harkins (Saint Louis University, Missouri, USA) for making available the MPC 9/3L-AH cell line and Dr. Cristina Plata (Universitat Pompeu Fabra, Barcelona, Spain) for technical assistance with MPC cells transfection. We thank Drs. Mike Seagar and Christian Lévêque (Inserm U641, Marseille, France) for antibodies. We are grateful to Dr. Emilio Carbone (University of Torino, Torino, Italy) for critical discussions.

NW was supported by fellowships from Alberta Heritage Foundation for Medical Research and from Hotchkiss Brain Institute. JMFF was funded by Spanish Ministry of Science and Innovation, Fondos Europeos de Desarrollo Regional (FEDER) Funds, and Plan E (Grant SAF2009-13182-C03-02), Fondo de Investigación Sanitaria (Red HERACLES RD06/0009) and Generalitat de Catalunya (Grant 2009SGR1369). LL was supported by VEGA 2/0195/10 grant. PL was supported by ANR-2006-Neuro35 and ANR-09-MNPS-035 grants. GWZ is funded by the Canadian Institutes of Health Research, is a Canada Research Chair and Scientist of the Alberta Heritage Foundation for Medical Research.

FIGURE LEGENDS

FIGURE 1. **$Ca_v3.2$ channel interacts with syntaxin-1A in central neurons.** *A*, Confocal images of nRT neurons permeabilized and stained for $Ca_v3.2$ (green) and syntaxin-1A (red). Overlaid images and colocalized pixels (in white) are shown. *B*, Intensity correlation analysis (ICA) plots of $Ca_v3.2$ and syntaxin-1A staining intensities against their respective (A-a)(B-b) values performed from the ROIs indicated in the overlaid image in (*A*). IQC = +0.31 and +0.38 for soma and neurite regions respectively. *C*, Co-immunoprecipitation of syntaxin-1A from rat brain homogenate with specific anti-$Ca_v3.1$, anti-$Ca_v3.2$ and anti-$Ca_v3.3$ antibodies.

FIGURE 2. **Syntaxin-1A modulates $Ca_v3.2$ channel inactivation.** *A*, Representative Ba^{2+} current traces recorded from a $Ca_v3.2$ (top panel) and $Ca_v3.2$/Stx-1A-expressing cell (bottom panel) in response to 150 ms depolarizing steps to -20 mV from a holding potential varied from -120 mV to -50 mV (*a* to *f*). *B*, Corresponding mean normalized steady-state inactivation curves for $Ca_v3.2$ (filled circles) and $Ca_v3.2$/Stx-1A-expressing cells (open circles). *C*, Plot of the mean shift values in the half-inactivation potential of $Ca_v3.2$ channel coexpressed with the different protein combinations indicated in the figure. *D*, Mean normalized activation curve for $Ca_v3.2$ (filled circles) and $Ca_v3.2$/Stx1A-expressing cells (open circles). Inset indicates the shift values in the half-activation potential produced upon coexpression of Stx1A or $Stx1A^{\Delta TM}$. Stx-1A, syntaxin-1A; BoNT/C, botulinium neurotoxin C1.

FIGURE 3. **Syntaxin-1A interacts within the carboxy-terminal domain of $Ca_v3.2$.** *A*, Schematic representation of the different constructs of intracellular regions of $Ca_v3.2$ used. *B*, Whole-cell Ba^{2+} currents (top panels) recorded in response to a 150 ms depolarizing step to -20 mV from a holding potential of -85 mV before (P1) and after (P2) a 5 sec hyperpolarizing pulse to -130 mV in a $Ca_v3.2$ (left panel), $Ca_v3.2$ / Stx-1A (middle panel) and $Ca_v3.2$ / Stx-1A / CD4-$Ca_v3.2^{Cter}$-expressing cell (right panel) and the corresponding mean plot of the current facilitation (I_{P2} / I_{P1}) (bottom panel). Note that the hyperpolarizing pulse produces a strong current facilitation in the presence of Stx-1A which is competitively and specifically abolished upon co-expression of the CD4-$Ca_v3.2^{Cter}$ construct. *C*, Confocal images of living COS cells showing the translocation of the EGFP-$Ca_v3.2^{Cter}$ construct (green) to the plasma membrane mediated by Stx-1A. Plasma membrane was stained with rhodamine labeled concanavalin A (ConA-Rhod, red). Overlaid images and pixel intensity profiles of crossed sections indicated by the white line are shown. Note that Stx-1A does not translocate EGFP-$Ca_v3.2^{II\text{-}III\ linker}$ fusion protein. *D*, Co-immunoprecipitation of the CD4-EGFP-$Ca_v3.2^{Cter}$ fusion protein from tsA-201 cells co-transfected with Stx-1A-Myc. The upper panel shows the immunoblot of CD4-EGFP-$Ca_v3.2^{Cter}$ fusion protein in the absence (-) and presence (+) of Stx-1A-Myc using an anti-GFP antibody. *Possible degradation of the CD4-EGFP-$Ca_v3.2^{Cter}$ fusion protein. The lower panel shows the results of the co-immunoprecipitation of the CD4-EGFP-$Ca_v3.2^{Cter}$ fusion protein with Stx-1A-Myc using an anti-Myc antibody. In the absence of Stx-1A-Myc the antibody alone is not able to immunoprecipitate the CD4-EGFP-$Ca_v3.2^{Cter}$ fusion protein.

FIGURE 4. **$Ca_v3.2$ channel induces voltage-dependent exocytosis.** *A*, Representative Ca^{2+} current traces recoded from MPC 9/3L-AH cells expressing $Ca_v3.2$ channel alone (top panel), and in combination with CD4-$Ca_v3.2^{Cter}$ (middle panel) or CD4-$Ca_v3.2^{II\text{-}II\ linker}$ (bottom panel) in response to a 100 ms long depolarizing step to -20 mV from a holding potential of -90 mV. These data show that T-type currents are functional in the presence of CD4-$Ca_v3.2^{Cter}$. *B*, Corresponding mean Ca^{2+} influx normalized by the whole-cell capacitance [Q_{Ca} density (pC/pF)] elicited by the 100 ms long depolarizing step to -20 mV. *C*, Capacitance traces plotted as a function of time from the same cells shown in (*A*). *D*, Corresponding mean exocytosis [ΔCm (fF)] normalized as a function of Ca^{2+} entry [Q_{Ca} density (pC/pF)].

FIGURE 5. **Expression of the CD4-EGFP-$Ca_v3.2^{Cter}$ fusion protein does not prevent exocytosis induced by intracellular calcium elevation.** *A*, Representative capacitance traces plotted as a function of time recorded from MPC 9/3L-AH cells expressing EGFP (black trace) or CD4-EGFP-$Ca_v3.2^{Cter}$ (light grey) in response to the superfusion of 1µM ionomycin (indicated by the arrow). A representative capacitance trace recorded from an EGFP-expressing cell in the absence of extracellular Ca^{2+} (EGFP - 0 Ca^{2+}) is also shown (dark grey). *B*, Corresponding mean exocytosis values [ΔCm (fF)] for EGFP (with (black) and without (dark grey) extracellular Ca^{2+}) and CD4-EGFP-$Ca_v3.2^{Cter}$-expressing cells (light grey). *C*, Corresponding time constant values (tau) of capacitance change obtained by fitting the rising phase of the traces by a single exponential function.

FIGURES

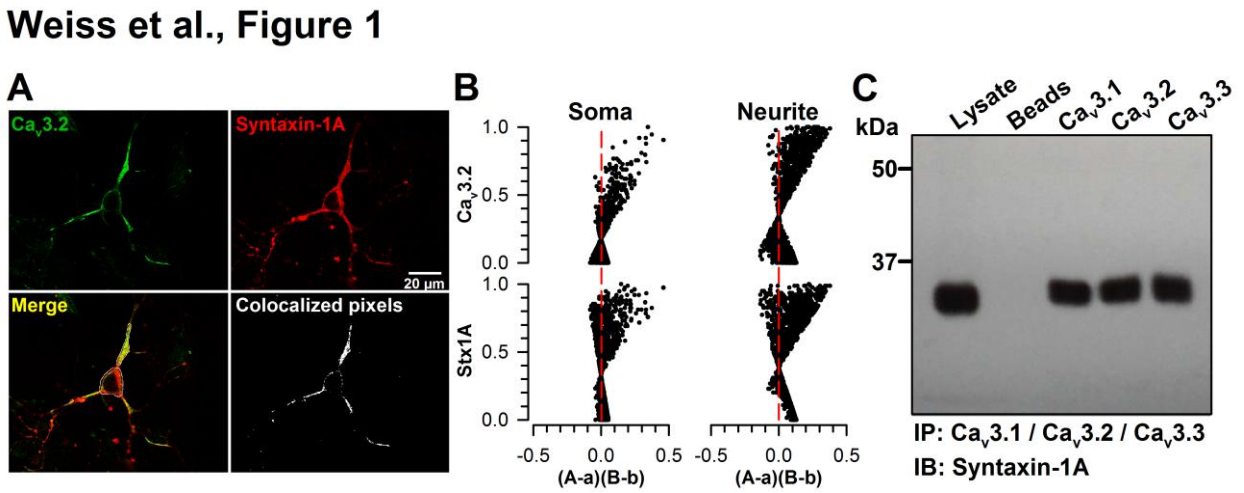
Weiss et al., Figure 1
A
Ca$_v$3.2
Syntaxin-1A
20 µm
Merge
Colocalized pixels
B
Soma
Neurite
Ca$_v$3.2
Stx1A
1.0
0.5
0.0
-0.5
0.0
0.5
(A-a)(B-b)
C
kDa
Lysate
Beads
Ca$_v$3.1
Ca$_v$3.2
Ca$_v$3.3
50
37
IP: Ca$_v$3.1 / Ca$_v$3.2 / Ca$_v$3.3
IB: Syntaxin-1A

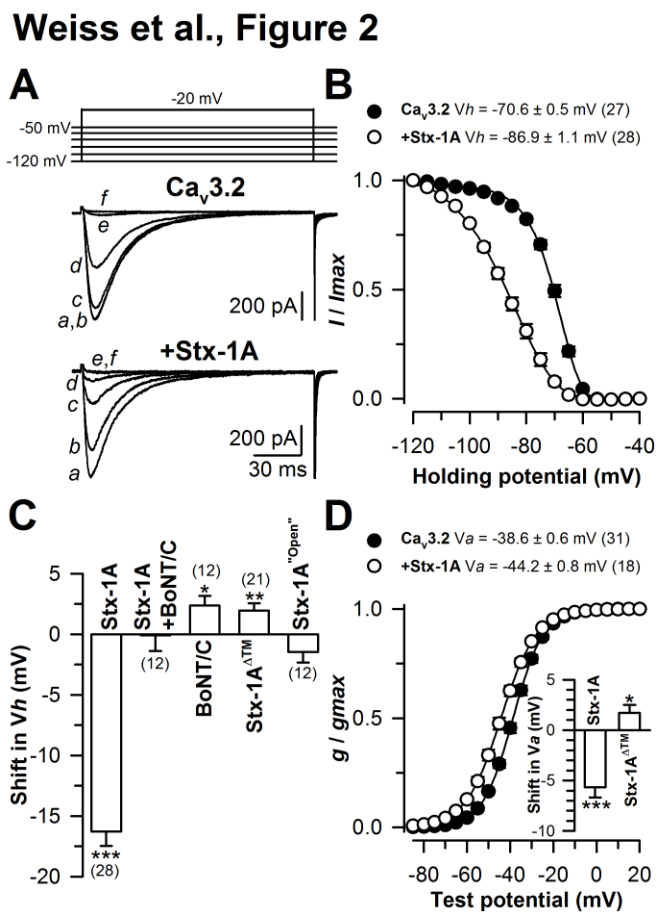
Weiss et al., Figure 2
A
-20 mV
-50 mV
-120 mV
Ca$_v$3.2
f
e
d
c
a,b
200 pA
+Stx-1A
e,f
d
c
b
a
200 pA
30 ms
B
Ca$_v$3.2 Vh = -70.6 ± 0.5 mV (27)
+Stx-1A Vh = -86.9 ± 1.1 mV (28)
I / Imax
1.0
0.5
0.0
-120 -100 -80 -60 -40
Holding potential (mV)
C
Shift in Vh (mV)
5
0
-5
-10
-15
-20
Stx-1A
Stx-1A +BoNT/C
BoNT/C
Stx-1A$^{\Delta TM}$
Stx-1A "Open"
(12)
*
(21)
**
(12)
(12)
***
(28)
D
Ca$_v$3.2 Va = -38.6 ± 0.6 mV (31)
+Stx-1A Va = -44.2 ± 0.8 mV (18)
g / gmax
1.0
0.5
0.0
-80 -60 -40 -20 0 20
Test potential (mV)
Shift in Va (mV)
5
0
-5
-10
Stx-1A
Stx-1A$^{\Delta TM}$
***
*

Weiss et al., Figure 3

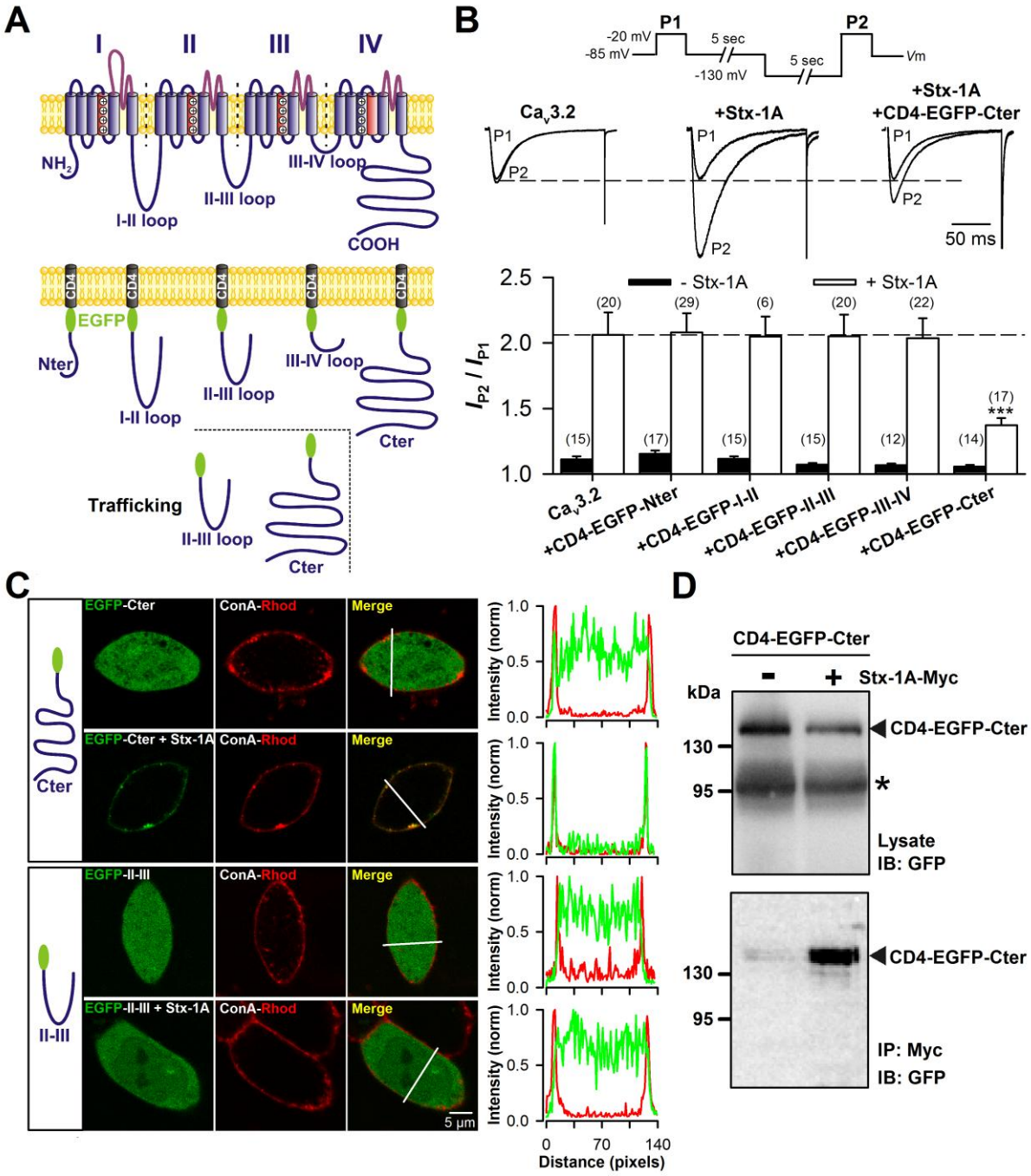

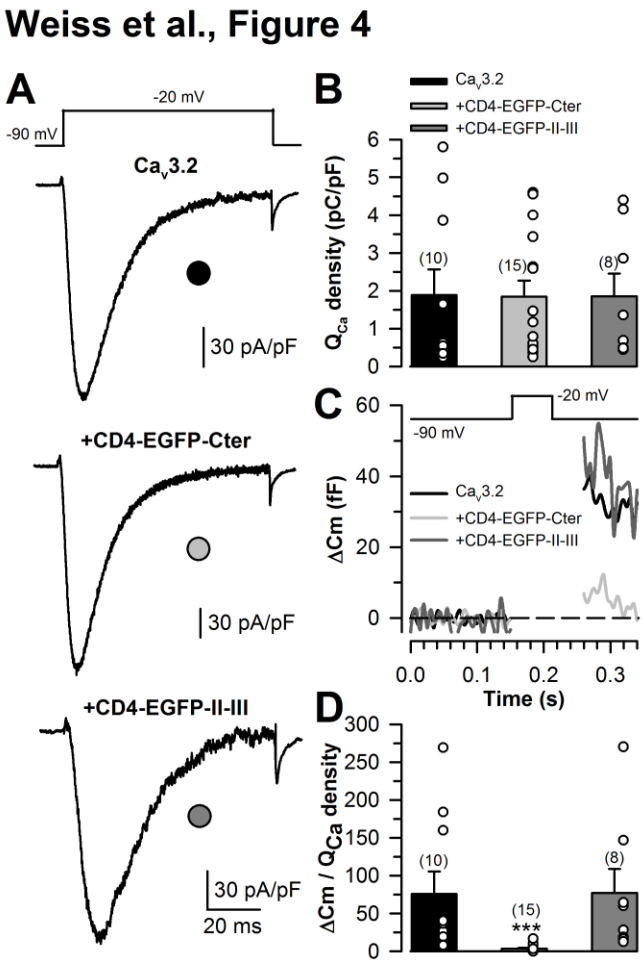
Weiss et al., Figure 4
A
-20 mV
-90 mV
Cav3.2
30 pA/pF
+CD4-EGFP-Cter
30 pA/pF
+CD4-EGFP-II-III
30 pA/pF
20 ms
B
Cav3.2
+CD4-EGFP-Cter
+CD4-EGFP-II-III
QCa density (pC/pF)
(10)
(15)
(8)
C
-20 mV
-90 mV
Cav3.2
+CD4-EGFP-Cter
+CD4-EGFP-II-III
ΔCm (fF)
Time (s)
D
ΔCm / QCa density
(10)
(15)
***
(8)

Weiss et al., Figure 5